[1,2.]Ramon de Paoli MENDES, [1.]Daniel Leon Ferreira POTTIE,
[2.]Leonardo Victor Silva MARTINS,
[1,3.] Maury Martins OLIVEIRA Jr , [1.]Lazaro Valentim DONADON

ANALYTIC STUDY IN FREQUENCY DOMAIN OF THE INTRODUCTION OF A HELMHOLTZ RESONATOR IN DIFFERENT DUCT POSITIONS OF A STEADY–STATE CYLINDRICAL WAVEGUIDES PROPAGATING PLANE WAVES

[1.]Postgraduate Program in Mechanical Engineering, Federal University of Minas Gerais, Belo Horizonte, BRAZIL
[2.]Advanced Refrigeration Group, Mechanical Engineering Department, Federal University of Minas Gerais, Belo Horizonte, BRAZIL
[3.]Thermometry Laboratory, Mechanical Engineering Department, Federal University of Minas Gerais, Belo Horizonte, BRAZIL

Abstract: The aim of this work is to synthesize in didactic character the theory about the frequency domain specific acoustic impedance variation as a function of the introduction of the Helmholtz Resonator for different positions along an acoustic cylindrical channel in which flat waves propagate in steady state. So that, provided the mathematical formulation and using the finite element technique it was possible to implement a Pseudo Code and a Scilab Code. A small prototype with a Helmholtz resonator designed to eliminate a frequency of 144,86 Hz was used to qualitatively verify the mathematical model, it was found that the results provided by the Code are in agreement with the experimental measurements. With the code it is possible to evaluate the effect of the resonator position along the acoustic duct.
Keywords: Acoustic; Helmholtz; Didactic

1. INTRODUCTION

A Helmholtz resonator consists of a cavity filled with air, attached to pipes or ducts through which sound is being propagated. The addition of the resonator results in sound attenuation in a determined frequency (Panton & Miller, 1975). A conceptual representation of such device is presented in the left–hand side of Figure 1, in which a Helmholtz resonator, with an internal volume V_0, length of neck X, which in the text will be treated as L, and cross section area of resonator neck S_v, can be attached to sound passing ducts.

Classical design guidelines states that if the sound wavelength (λ) is significantly larger than the dimensions L, $S_v^{1/2}$ and $V_0^{1/3}$ (Tang & Sirignano, 1973), the air mass (m) inside the resonator neck propagates the sound, compressing the air inside the cavity which, in turn, acts as a spring, opposing this movement (Vér & Benarek, 1992). This results in the appearance of a restoring force. The energy dissipation inside the resonator cavity acts as a damper. In this sense, a Helmholtz resonator can be modelled as a mass spring damper system, as shown in Figure 1, RHS.

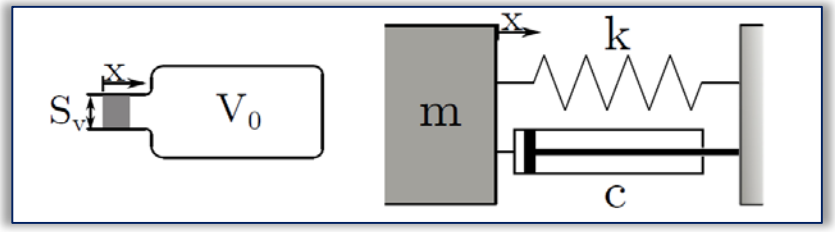

Figure 1: Helmholtz resonator dimensions and modelling as a mass spring damper system

ANNALS of Faculty Engineering Hunedoara – International Journal of Engineering
ISSN 1584 - 2665 (printed version); ISSN 2601 - 2332 (online); ISSN-L 1584 - 2665
Universitatea Politehnica Timişoara

This design procedure also considers that only the total cavity volume V_0 is important, not the shape of the resonator itself (Lamb, 1960). In another study, however, Alster (Alster, 1972) showed that the resonator shape does have an influence on the sound attenuating capacity. The error associated with the consideration of the volume as a single design parameter is usually around 9% (Alster, 1972). However, in this paper will be considered the classical procedure.

When a Helmholtz resonator is attached to a Waveguides in which sound is being transmitted, the air contained in the device neck resonates in the same frequency as the main sound source. For instance, this device can be installed to muffle noises generated by automotive vehicles exhaust systems ((Pereira, 2008), (Yasuda, Wu, Nakagawa, & Nagamura, 2013), (Song & Cho , 2017)).

Waveguides are structures whose function is to guide the waves (either mechanical or electromagnetic) in a certain direction (Collin, 1990). Among the mechanical waves, sound waves are particularly important due to its wide range of applications. When propagating through a cylindrical duct (as presented in Figure 2) in a certain frequency and intensity range, sound can lead to discomfort and hearing loss. Therefore, adding filtering and attenuating elements in these conditions are not only desired, but frequently a requirement.

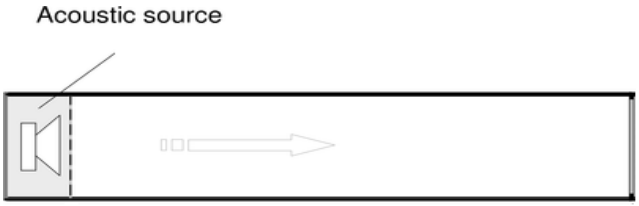

Figure 2: Cylindrical Waveguide (Weyna, Mickiewicz, Pyla, & Jablonski , 2013)

Inside cylindrical ducts, sound can travel in different modes, as a function of frequency. In order to determine how the sound will travel, it is necessary to solve the wave equation, in cylindrical coordinates, Equation (1).

$$\frac{1}{C^2}\cdot\frac{\partial^2 u}{\partial t^2}=\frac{\partial^2 \rho}{\partial \rho^2}+\frac{1}{\rho}\cdot\frac{\partial u}{\partial \rho}+\frac{1}{\rho^2}\cdot\frac{\partial^2 u}{\partial \phi^2}+\frac{\partial^2 u}{\partial x^2} \quad (1)$$

Where ρ is the air density, u is a transport variable, such as pressure or velocity, and C is the local speed of sound. The solution of Equation (1) results in the vibration mode as a function of the type (n) and order (ṁ) of the Bessel function, and its derivative J̇ (Lopez, 2014).

Table 1: Vibrational modes resultant of solving the wave equation given by Bessel equation parameters.

Order	$\dot{m}=0$	$\dot{m}=1$	$\dot{m}=2$
Derivative	$\dot{J}_0=0$	$\dot{J}_1=0$	$\dot{J}_2=0$
n=0	0	1.84	3.05
n=1	3.84	5.33	6.71
n=2	7.02	8.44	9.97

Different values of J̇ , ṁ and n result on sound propagation in different modes. In Figure 3, the first three vibrational modes are shown. For the first mode ($\dot{m}=1$ and $n=0$), in which sound travels as a plane wave, return a value equal to 1.84. This value can be used to relate the angular wave number k and the duct radius r as follows.

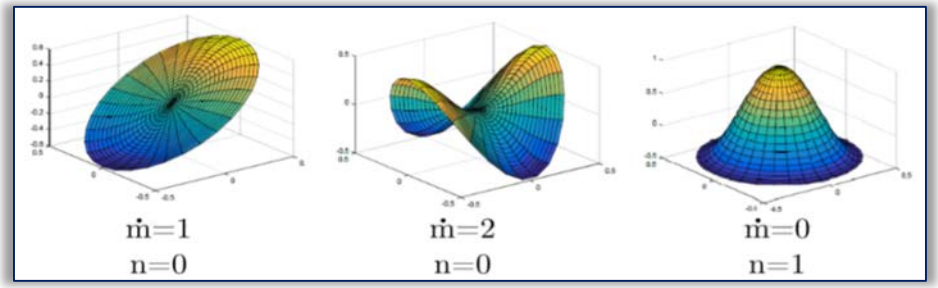

Figure 3: First, second and third vibrational mode for a cylindrical waveguide, and their respective ṁ and n values

$$k\cdot r=1.84 \quad (2)$$

Where the angular wave number k is given in m^{-1} whilst the duct diameter is in meters. In this sense, the cut–off frequency, defined as the higher frequency in which sound vibrates in the first mode, can be determined through Equation 3.

$$f_c\leq\frac{1.84}{2\cdot\pi\cdot r}\cdot C \quad (3)$$

where the cut–off frequency is given in Hz and the local sound speed, C, in $m.s^{-1}$. Accordance to Equation 3 is a keystone in the design process explored in this paper. The methodology hereby presented is valid only for plane waves inside a cylindrical duct, and, for this reason, only frequencies smaller than f_c will be studied. (Kinsler, Frey , Coppens, & Sanders, 2000)

By adding a Helmholtz resonator through a sound propagating duct, the acoustic impedance in the design frequency will reduce significantly. The acoustic impedance is defined as the opposition presented by the system to the passage of a wave (Dourado, 2004), and can be calculated as the ratio between pressure and velocity (Kinsler, Frey , Coppens, & Sanders, 2000). As the velocity is constant and equal to the local speed of sound, reducing the impedance decreases the pressure in the duct outlet. As the sound intensity, in $W.m^{-2}$, is given by the product of pressure and velocity, it also decreases, leading to the desired acoustic attenuation.

In this work the use of a single Helmholtz Resonator will be studied in different positions of a cylindrical duct in which flat waves are propagating in steady state.

In the methodology section the mathematical model, which consists of the equation in the frequency domain of the mechanics associated to the Resonator and the discretization of the duct and the resonator in finite elements, in order to obtain the matrix that describes the physical behavior of the system, will be presented. Next, in the Numeric Study section, we will present the use of the resonator at four locations along the cylindrical duct and the results associated with the use of the described methodology. In the Experimental Study section, the construction and use of a bench will be described in order to ratify the results. In Appendix A one pseudo code was provided and in Appendix B one code em Scilab.

2. METHODOLOGY

— Theoretical formulation: Resonator design frequency and acoustic impedance

The considered system comprises of a cylindrical duct with a Helmholtz resonator attached, similar to Figure 1. The air in the resonator neck vibrates due to the sound propagating in the main duct, and interacts with the air stored in the cavity. This interaction was modelled after a conventional mass spring damper system, described as follows:

$$m \cdot \ddot{x} + c \cdot \dot{x} + k \cdot x = F(t) \tag{4}$$

In which c is the damping coefficient $[kg.s^{-1}]$, k is the spring elastic constant $[N.m^{-1}]$ and F(t) is the external force applied to the system [N]. Considering this force as the input and a displacement D(t) as output for Equation 4, it is possible to apply the Laplace transform (Williams, 1973), resulting in the following transfer function:

$$\frac{D(s)}{F(s)} = \frac{1}{m \cdot s^2 + c \cdot s + k} \tag{5}$$

While the Fourier transform only takes into account the imaginary axis in the 2–D complex plane, the Laplace transfer considers both real and complex axis (Seo & Chen, 1986). Thus, the Fourier transform is a particular case of the Laplace transform, which considers only the complex part of the variable s. If s is defined as:

$$s = \sigma + j \cdot \omega \tag{6}$$

where ω is the angular frequency, given in s^{-1}. Then, it is possible to take Im(s) = ωj and replace it on Equation 5, shifting it from a time base to frequency base. Thus, by replacing s = ωj,

$$\frac{D(j\omega)}{F(j\omega)} = \frac{1}{m \cdot (j\omega)^2 + c \cdot j\omega + k_s} \tag{7}$$

In order to obtain the velocity, we simply take the first derivative of the displacement in respect to time, then transform it to the frequency domain once again by considering s = ωj, as follows:

$$D(s) = \frac{V(s)}{v} \Longrightarrow D(\omega \cdot j) = \frac{V(\omega \cdot j)}{(\omega \cdot j)} \tag{8}$$

By replacing this definition in Equation 7, it is possible to define the mechanical impedance in the frequency domain as

$$\frac{F(\omega \cdot j)}{V(\omega \cdot j)} = c - j \cdot \left(\frac{k_s}{\omega} - \omega \cdot m\right) \tag{9}$$

In Equation 9, it is clearly noticeable that the real component of the mechanical impedance represents the dampening.

For a small distance after leaving the main duct, the air keeps on behaving as if it were inside the waveguide (Gerges, 2000). So, in the design process of a Helmholtz resonator, it is necessary to consider a neck length slightly larger than the actual dimension L_{eq}. In this sense, Porges (Porges, 1977) and Kinsley (Kinsler, Frey , Coppens, & Sanders, 2000) performed experimental studies on the subject, and found that for flanged pipes, equivalent to the resonator neck, L_{eq} can be expressed as

$$L_{eq} = L + 2 \cdot 0.85 \cdot r_v = L + 1.7 \cdot r_v \quad (10)$$

In which L is the actual neck length and r_v is the neck radius, all given in m. If the neck is not flanged, the latter part of Equation 10 must be replaced by 0.6 r. The air mass contained in the resonator neck can be defined as

$$m = \rho \cdot S_v \cdot (L + 1.7 \cdot r_v) \quad (11)$$

In which ρ is given in $kg.m^{-3}$. The force driving the air through the resonator neck can be expressed as:

$$F(x) = m \cdot \ddot{x} \quad (12)$$

By replacing Equation 11 into Equation 12,

$$F(x) = \rho_0 \cdot S_v \cdot (L + 1.7 \cdot r) \cdot \ddot{x} \quad (13)$$

The dampening effect is a result of the sound propagating out of the main duct into the atmosphere, and it can be expressed as the real component of the ratio between the sound impedance and the product of air density, speed of sound and duct cross section (Equation 14 and Equation 15) (Kinsler, Frey , Coppens, & Sanders, 2000) This ratio results in different values whether the duct is flanged or not (Equation14 and 15, respectively) (Kinsler, Frey , Coppens, & Sanders, 2000).

$$\frac{Z_{ml}}{\rho_0 \cdot C \cdot S_v} = \frac{1}{2} \cdot (k \cdot r^2) \quad (14)$$

$$\frac{Z_{ml}}{\rho_0 \cdot C \cdot S_v} = \frac{1}{4} \cdot (k \cdot r^2) \quad (15)$$

Thus, for flanged ducts, the dampening force can be expressed as the product between the dampening coefficient and the velocity:

$$F_c = Z_{ml} \cdot \dot{x} = c \cdot \dot{x} = \rho_0 \cdot C \cdot S_v \cdot \frac{1}{2}(k \cdot r^2) \cdot \dot{x} \quad (16)$$

Considering the resonator neck, the air movement inside it can be considered as a piston compressing a cylinder. Therefore, if a displacement x occurs in the neck, the entirety of the volume V_0 is reduced by a factor $\Delta V = x \cdot S_v$.

It is possible to define the acoustic condensation, s_c, as the change in the air density caused by the sound propagation. This condensation can also be rewritten as:

$$s_c = \frac{\rho - p_0}{p_0} = \frac{\Delta V}{V} = \frac{S_v \cdot x}{V} \quad (17)$$

From (Kinsler, Frey , Coppens, & Sanders, 2000), it is possible to define the acoustic pressure as the product between Bulk module, β, and the acoustic condensation

$$p(t) = \beta \cdot \frac{S_v \cdot x}{V} \quad (18)$$

The local speed of sound can be obtained as the square root of the ratio between Bulk module and the local air density (Kinsler, Frey , Coppens, & Sanders, 2000).

$$C^2 = \frac{\beta}{\rho_0} \quad (19)$$

By combining Equations 18 and 19 it is possible to determine the force applied by the air mass in the resonator neck as the product between pressure, $p(t)$, and the neck area, S_v

$$F = S_v \cdot p(t) = \rho_0 \cdot C^2 \cdot \frac{S_v^2}{V} \cdot x \quad (20)$$

This force can be modelled as a spring restoring force acting upon the resonator cavity air volume. Therefore, from Equation 20, it is possible to define an equivalent spring elastic constant, k_{eq},

$$k_{eq} = \rho_0 \cdot C^2 \cdot \frac{S_v^2}{V} \quad (21)$$

Thus, the natural frequency resulting from this restoring spring–like force can be obtained as the square root of the ratio between the equivalent spring constant and the resonator neck air mass. From Equation 11 and Equation 21, the natural frequency can be written as

$$\omega^2 = \frac{k_{eq}}{m} = \frac{\rho_0 \cdot C^2 \cdot \frac{S_v^2}{V}}{\rho_0 \cdot S_v \cdot L_{eq}} \tag{22}$$

which leads to

$$\omega^2 = \frac{C^2 \cdot S_v}{V \cdot L_{eq}} \tag{23}$$

It is more convenient to convert Equation 23 to be expressed in Hz. Thus, Equation 23 can be rewritten as

$$f = \frac{1}{2 \cdot \pi} \cdot C \cdot \left(\frac{S_v}{V \cdot L_{eq}}\right)^{\frac{1}{2}} \tag{24}$$

Finally, the acoustic impedance caused by attaching a Helmholtz resonator to a duct can be obtained by analysing Equation 9. The dampening coefficient, c, referring to the real component of Equation 9, is given by Equation 16. On the other hand, the imaginary portion of Equation 9 is given by Equation 21 and Equation 11, as follows

$$\frac{F(\omega \cdot j)}{V(\omega \cdot j)} = \rho_0 \cdot C \cdot S_v \cdot \frac{1}{2} \cdot (k \cdot r)^2 - j \cdot \left(\frac{\rho_0 \cdot C^2 \cdot S_v^2}{\omega \cdot V} - \omega \cdot \rho_0 \cdot S_v \cdot L_{eq}\right) \tag{25}$$

$$Z_{Ress} = \rho_0 \cdot C \cdot S_v \cdot \left[\left(\frac{1}{2} \cdot (k \cdot r)^2\right) - j \cdot \left(\frac{S_v}{k \cdot V} - k \cdot L_{eq}\right)\right] \tag{26}$$

— Acoustic spectral element

The general differential equation that describes the sound propagation, in a cylindrical coordinate system, is presented in Equation 1. Considering a steady–state condition and an incompressible flow in the axial direction, Equation 1 can be simplified to

$$\frac{\partial^2 u}{\partial t^2} - C^2 \cdot \left(\frac{\partial^2 u}{\partial x^2}\right) = 0 \tag{27}$$

Again, u can be any transport variable. Considering u to be equal to pressure p, and using the Fourier method for variable separation (Boyce & DiPrima, 2010), it is possible to define a pressure function along the duct length L for the pressure, given the angular frequency (ω) and the wave number k (Kinsler, Frey , Coppens, & Sanders, 2000).

$$k = \frac{\omega}{C} \tag{28}$$

$$P(x, \omega) = A \cdot e^{-j \cdot k \cdot x} + B \cdot e^{j \cdot k \cdot x} \tag{29}$$

Considering a duct segment, with length L, cross section area S and pressure at inlet ($x_1 = 0$) and outlet ($x_2 = L$),

$$P_1 = P_{0,\omega} = A + B \tag{30}$$

$$P_2 = P_{L,\omega} = A \cdot e^{-j \cdot k \cdot L} + B \cdot e^{j \cdot k \cdot L} \tag{31}$$

It is possible to combine Equation 30 and 31 to solve for the constants A and B

$$B = P_1 - A \tag{32}$$

$$P_2 = P_{L,\omega} = A \cdot e^{-j \cdot k \cdot L} + (P_1 - A) \cdot e^{j \cdot k \cdot L} \tag{33}$$

A variable Δ can be defined as

$$\Delta = e^{-j \cdot k \cdot L} - e^{j \cdot k \cdot L} \tag{34}$$

By combining Equations 30 through 34 into the definition presented in Equation 29, it is possible to define a relationship for the pressure at any point in the main duct as

$$P(x, \omega) = \left[\frac{P_2 - P_1 \cdot e^{j \cdot k \cdot l}}{\Delta}\right] \cdot e^{-j \cdot k \cdot x} + \left[\frac{P_1 \cdot e^{-j \cdot k \cdot l} - P_2}{\Delta}\right] \cdot e^{j \cdot k \cdot x} \tag{35}$$

Rearranging Equation 35 as the net pressure difference between any two points in the duct

$$\Delta P_{x,\omega} = P_1 \cdot \left(e^{-j \cdot k \cdot (L-x)} - e^{j \cdot k \cdot (L-x)}\right) + P_2 \cdot \left(e^{-j \cdot k \cdot x} - e^{j \cdot k \cdot x}\right) \tag{36}$$

The volume velocity is defined as the product between the cross section and its average air velocity. For plane waves, it can be obtained from Equation 37 [12]

$$U(x,\omega) = S \cdot u(z,\omega) = \frac{J \cdot S}{\omega \cdot \rho_0} \cdot \frac{\partial P_{x,\omega}}{\partial x} \quad (37)$$

Considering the derivative of the pressure with respect to x:

$$U(x,\omega) = \frac{-S}{\Delta \cdot \rho_0 \cdot C} \cdot \left(P_1 \cdot \left(e^{-j\cdot k\cdot(L-x)} + e^{j\cdot k\cdot(L-x)}\right) - P_2 \cdot \left(e^{-j\cdot k\cdot x} + e^{j\cdot k\cdot x}\right)\right) \quad (38)$$

The volume velocities at the inlet, U_1, and outlet, U_2 can be expressed as a function of the pressures at their locations (Equation 39 and Equation 41)

$$U_1 = U_{0,\omega} = \frac{-S}{\Delta \cdot \rho_0 \cdot C} \cdot \left(P_1 \cdot \left(e^{-j\cdot k\cdot L} + e^{j\cdot k\cdot L}\right) - 2 \cdot P_2\right) \quad (39)$$

$$U_2 = -U_{L,\omega} = \frac{S}{\Delta \cdot \rho_0 \cdot C} \cdot \left(2 \cdot P_1 - P_2 \cdot \left(e^{-j\cdot k\cdot L} + e^{j\cdot k\cdot L}\right)\right) \quad (40)$$

$$U_2 = \frac{S}{\Delta \cdot \rho_0 \cdot C} \cdot (2 \cdot P_1 - \Delta \cdot P_2) \quad (41)$$

It is convenient to represent the volume velocities equations as matrices. By combining Equation 38 and Equation 40, it is possible to express the velocities U_1 and U_2 as a function of P_1 and P_2.

$$\begin{bmatrix} U_1 \\ U_2 \end{bmatrix} = \begin{bmatrix} K11 & K12 \\ K21 & K22 + \frac{S^2}{Z_{ml}} \end{bmatrix} \cdot \begin{bmatrix} P_1 \\ P_2 \end{bmatrix} \quad (42)$$

In Equation 41, it is worth mentioning that the presence of $\frac{S^2}{Z_{ml}}$ added to the element K22 is to take into account the impedance between the duct and the open–ended section at x = L, as expressed by Equation 15. In an analogous manner, when the impedance imposed by the resonator is analysed, $\frac{S^2}{Z_{ml}}$ must be replaced by $\frac{{S_v}^2}{Z_{Ress}}$. Finally, the K elements can be expressed as

$$K11 = -\left[\frac{S}{\rho_0 \cdot C \cdot (e^{-j\cdot k\cdot L} - e^{j\cdot k\cdot L})}\right] \cdot \left(e^{-j\cdot k\cdot L} + e^{j\cdot k\cdot L}\right) \quad (43)$$

$$K12 = -\left[\frac{S}{\rho_0 \cdot C \cdot (e^{-j\cdot k\cdot L} - e^{j\cdot k\cdot L})}\right] \cdot (-2) \quad (44)$$

$$K21 = -\left[\frac{S}{\rho_0 \cdot C \cdot (e^{-j\cdot k\cdot L} - e^{j\cdot k\cdot L})}\right] \cdot (-2) \quad (45)$$

$$K22 = -\left[\frac{S}{\rho_0 \cdot C \cdot (e^{-j\cdot k\cdot L} - e^{j\cdot k\cdot L})}\right] \cdot \left(e^{-j\cdot k\cdot L} + e^{j\cdot k\cdot L}\right) \quad (46)$$

In order to analyse the acoustic impedance between the input and output of the element, the matrix needs to be divided by the input velocity and the velocities inside the duct considered as zero.

$$\begin{bmatrix} \frac{P_1}{U_1} \\ \frac{P_2}{U_1} \end{bmatrix} = \begin{bmatrix} K11 & K12 \\ K21 & K22 + \frac{S^2}{Z_{ml}} \end{bmatrix}^{-1} \cdot \begin{bmatrix} 1 \\ 0 \end{bmatrix} \quad (47)$$

3. NUMERIC STUDY

The case study consists of two parts. In the first, the mathematical model presented in the previous section was used to simulate the effects of the attachment of a Helmholtz resonator to a cylindrical waveguide. In the second part, an experimental setup was built to validate the simulation results.

The case studied consisted of a Helmholtz resonator attached to a cylindrical duct whose main constructive parameters are presented in Figure 4.

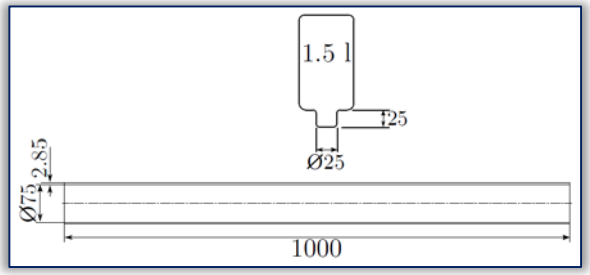

Figure 4: Waveguide and resonator dimensions

The mathematical model presented in the previous section was implemented using Scilab (ESI Group, 2019) (see Annex 1). The sound source position was set in the left–hand side opening, and the output sound impedance in the opposite end. The resonator influence was studied in four different positions: (1) 40 mm; (2) 380 mm; (3) 690 mm and (4) 970 mm from the sound generator. These scenarios are presented in Figure 5.

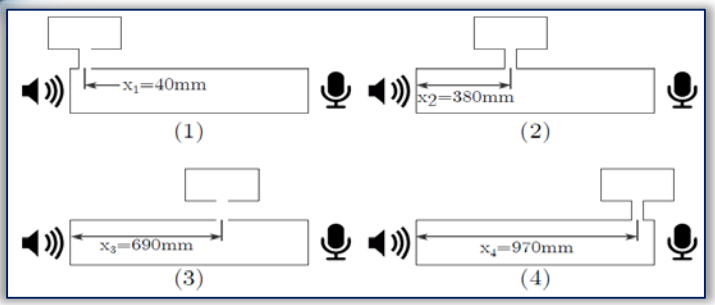

Figure 5: Four different scenarios studied in the numerical simulation of a Helmholtz resonator

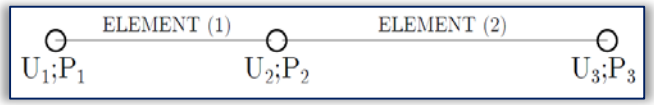

Figure 6: Main acoustic duct discretized into finite elements

The cylindrical waveguide was discretized into two elements in order to apply the proposed methodology. The first element starts at the left–hand side of the duct, at the sound source, and finishes at the resonator attaching point to the main duct. At this point, the acoustic impedance imposed by the resonator will be taken into account (Equation 26). The output of the first element will be used as input for the second element, starting at the same point and ending at the right–hand side open end of the duct. At the right–hand side of element (2) the acoustic impedance to the surrounding atmosphere was also added (Equation 15). Figure 6 depicts the discretized elements, the nodal points, degrees of freedom and pressures.

Then, Equation 41 is applied to each element of the discretized system. For element (1), the impedance caused by the Helmholtz resonator, $\frac{S^2}{Z_{ress}}$, is added to element K22. In an analog way, for element (2) the impedance $\frac{S^2}{Z_{ml}}$ between the duct and the surroundings is considered.

$$\begin{bmatrix} U_1 \\ U_2 \end{bmatrix} = \begin{bmatrix} K11^1 & K12^1 \\ K21^1 & K22^1 + \frac{S^2}{Z_{Ress}} \end{bmatrix} \cdot \begin{bmatrix} P_1 \\ P_2 \end{bmatrix} \tag{48}$$

$$\begin{bmatrix} U_2 \\ U_3 \end{bmatrix} = \begin{bmatrix} K11^2 & K12^2 \\ K21^2 & K22^2 + \frac{S^2}{Z_{Ress}} \end{bmatrix} \cdot \begin{bmatrix} P_2 \\ P_3 \end{bmatrix} \tag{49}$$

It is possible to combine Equations 47 and 48 to obtain the global stiffness matrix. Here, it is important to mention that the superscript "1" refers to Equation 47, while the superscript "2" refers to Equation 48.

$$\begin{bmatrix} U_1 \\ U_2 \\ U_3 \end{bmatrix} = \begin{bmatrix} K11^1 & K12^1 & 0 \\ K21^1 & K_{EQ1} & K12^2 \\ 0 & K21^2 & \left(K22^2 + \frac{S^2}{Z_{Ress}}\right) \end{bmatrix} \cdot \begin{bmatrix} P_1 \\ P_2 \\ P_3 \end{bmatrix} \tag{50}$$

$$K_{EQ1} = \left(K11^1 + K22^1 + \frac{S^2}{Z_{Ress}}\right) \tag{51}$$

It is possible to divide both sides of Equation 49 by the inlet velocity U_1. This way, the pressure column matrix becomes the acoustic impedance. Furthermore, velocities U_2 and U_3 are considered zero to be able to assess the impedance output as a function of the input velocity U_1 exclusively. Then rewriting Equation 49 to express the impedance as a function of the input velocity (U_1).

$$\begin{bmatrix} \frac{P_1}{U_1} \\ \frac{P_2}{U_1} \\ \frac{P_3}{U_1} \end{bmatrix} = \begin{bmatrix} K11^1 & K12^1 & 0 \\ K21^1 & K_{EQ2} & K12^2 \\ 0 & K21^2 & \left(K22^2 + \frac{S^2}{Z_{Ress}}\right) \end{bmatrix}^{-1} \cdot \begin{bmatrix} 1 \\ 0 \\ 0 \end{bmatrix} \tag{52}$$

$$K_{EQ2} = \left(K21^1 + K22^1 + \frac{S_v^2}{Z_{Ress}}\right) \tag{53}$$

To evaluate the resonator response over a wide range of frequencies, an iterative method was used, varying the frequency in unitary steps from 0 up to 1,500 Hz. The acoustic impedance at the duct output was registered in each case.

A Helmholtz resonator with an internal volume of 1.5ℓ was chosen. This internal volume V resulted in a design frequency equal to 144.86 Hz (Equation 24), whose value is below the cut–off frequency (2 kHz). Firstly, however, it is necessary to analyse the acoustic impedance response without the resonator, in order to properly assess its effect. So, Figure 7 presents the impedance output for a given input velocity (U_1) for the duct presented in Figure 4, without the resonator.

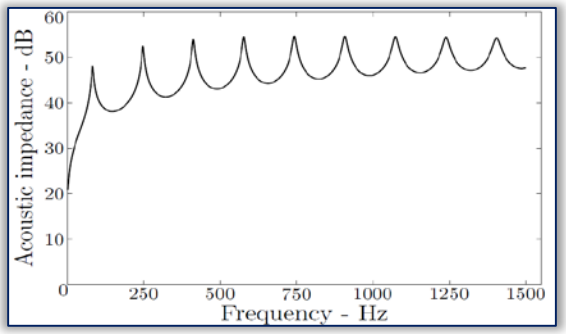

Figure 7: Acoustic impedance at the output of element (2) without the Helmholtz resonator

In Figure 7 it is possible to notice that the acoustic impedance is well behaved across the studied frequency range if the resonator is not utilized. The impact of the resonator on the acoustic impedance can be seen in Figure 8.

From Figure 8 it is clearly visible the profound effect the resonator has on the output acoustic impedance. When the resonator is placed 40 mm from the sound source, the attenuation occurs mainly on the design frequency. When the resonator is not present, the acoustic impedance for the design frequency is 38.23 dB, reducing to 9.54 dB for case (a).

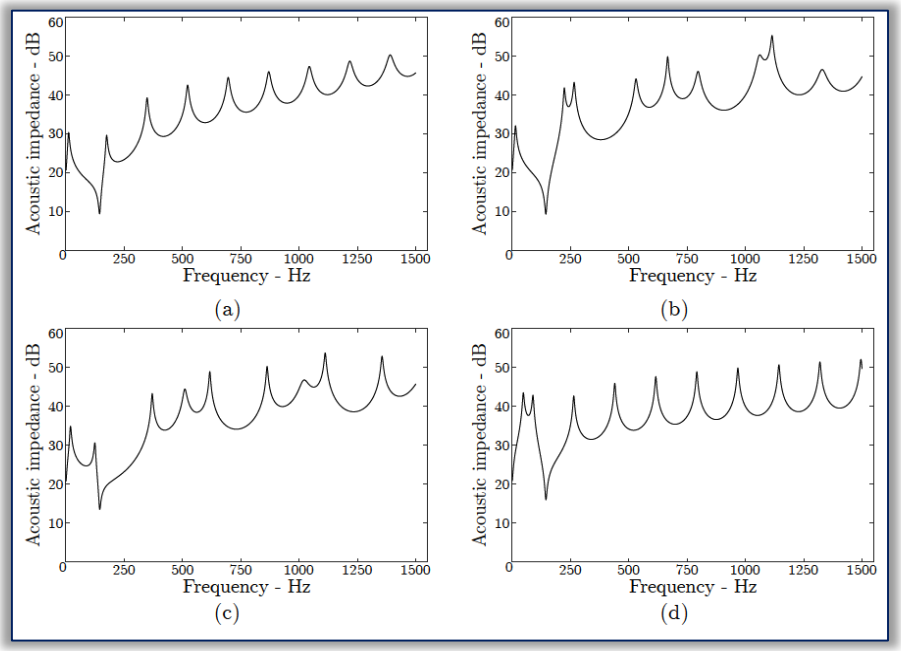

Figure 08: Acoustic impedance at the output of element (2) for each studied case: (a) 40 mm; (b) 380 mm; (c) 690 mm and (d) 970 mm from the sound source.

The second scenario, in which the resonator was placed 380 mm from the sound source (b) resulted in a similar sound impedance in the design point, 9.46 dB. However, the effect on higher frequencies greatly increased. The average impedance in this case was 37.01 dB, compared to the 46.07 dB found when the resonator was not installed and 35.72 dB in case (a).

In Figure 8 case (c), the effects of placing the resonator 690 mm from the sound source are similar to case (b). A slight increase in the average impedance is noticeable, 37.11 dB, however, when the design frequency (f = 144 Hz) is analysed, the results show a reduction in the attenuation, 14.01 dB. Lastly, in case (d) the effects of the resonator are greatly diminished, resembling the results presented in Figure 07, when the device was not present. Nevertheless, in the design frequency the desired attenuation was obtained, resulting in an acoustic impedance of 16.31 Hz. For clarity and comparison sake, there results were summarized in Table 2.

Table 2: Summary of average and local (at f=144Hz) acoustic impedance (dB) for different positions of the resonator: (a) 40 mm; (b) 380 mm; (c) 690 mm and (d) 970 mm from the sound source.

	Without	Case			
		(a)	(b)	(c)	(d)
Average	46.07	35.07	37.01	37.11	37.59
f = 144 Hz	38.23	9.54	9.46	14.01	16.31

4. EXPERIMENTAL STUDY

An experimental setup was built to match the parameters set in the numerical study. For that purpose, a 1 m length, diameter of 75 mm PVC duct was used, drilled at the same positions as presented in Sec 3.1 to which a Helmholtz resonator was to be attached. A speaker was placed in the left–hand side of the duct, whilst on the opposite end, a KY–038 Arduino sound sensor was placed, connected to a NI–6211 USB DAQ system. The setup can be seen in Figure 09. The sound signal was generated using a specific software at the design frequency (f=144,86 Hz). Differently from the numerical study, in which a wide range of frequencies responses were obtained, the experimental analysis was restricted to the design frequency only. The sound sensor used in this study produced an analog 0–5 V output, depending on the sound intensity. The analog voltage output was recorded, and later converted back to dB values, which are presented in Table 3.

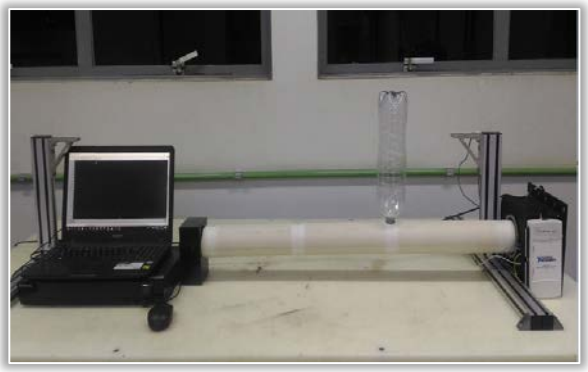

Figure 9: Test bench built for the experimental validation of the numeric study

Table 3: Average sound intensity at f=144Hz for experimental numeral study for different positions of measurements: (a) 40 mm; (b) 380 mm; (c) 690 mm and (d) 970 mm from the sound source.

	Case			
	(a)	(b)	(c)	(d)
Without Resonator (average) [dB]	72.3	72.3	72.3	72.3
With Resonator (average) [dB]	65	60.7	57.6	69.4

From Table 3 it is possible to see an average reduction of 12% in the output sound intensity due effect of the resonator. Positions (b) and (c) returned the best results, attenuating the output sound intensity by 11.6 and 14.7 dB, respectively.

5. CONCLUSIONS

This paper presents a thorough analysis of the design process of a Helmholtz resonator used to muffle plane sound waves propagating in a cylindrical waveguide. The analysis was divided into four sections. In the first, was the introduction, the second was the theoretical formulation, which included a finite element discretization, was described in detail. The mathematical model consisted in dividing the waveguide into elements, whose common node coincided with the resonator attaching point. The elements were approximated by a mass spring damper system, resulting in a global stiffness matrix.

The third part consisted in applying the methodology in a numerical study considering a particular case, simulating the effects of adding a Helmholtz resonator to a duct at four different locations. The numerical results have shown that the resonator attenuates the sound not only at the design frequency, but also over a wide range of frequencies. An average attenuation of 12% was obtained, with the resonator at positions (b) and (c), more central locations, achieving an average of 18%. At the design frequency the attenuation was around.

The fourth and last part consisted in an experimental study for validation of the numerical analysis. A contraption was built with the same parameters as the simulation parameters. However, the experimental results did not return attenuation levels as high as the numerical model. Finally, it is important stress that the objective of this paper is not do a quantitative analysis, but provide a synthesis of a qualitative analysis regarding the addiction of the Helmholtz resonator at different positions.

Acknowledgments

The authors would like to gratefully acknowledge the financial support provided by CAPES and CNPq.

Nomenclature

C	Damping coefficient, $kg.s^{-1}$	u	Transport variable
C	Local speed of sound, $m.s^{-1}$	V_0	Volume, m^3
D	Diameter, m	x	Spring elongation, m
F	Force, N	$\dot{x}$	Linear velocity, $m.s^{-1}$
f	Frequency, Hz	$\ddot{x}$	Linear acceleration, $m.s^{-2}$
f_c	Cut–off frequency, Hz	Z	Impedance
J	Bessel function	Z_{ml}	Radiation impedance
j	Bessel function derivative	Z_{Ress}	Acoustic impedance

j	Imaginary unit		
k	Angular wavenumber, m^{-1}	Greeks	
k_s	Spring elastic constant, $N.m^{-1}$	β	Bulk module
L	Length of the neck, m	ρ	Fluid density, $kg.m^{-3}$
m	Air mass, kg	ρ_0	Fluid density at ambient condition, $kg.m^{-3}$
$\dot{m}$	Bessel function order	λ	Sound wavelenght
n	Bessel function kind	ω	Angular frequency, s^{-1}
P	Pressure, Pa	σ	Real unit
r	Radius, m		
S	Cross section area, m^2	Subscripts	
s	Laplace transform complex variable	eq	equivalent
s_c	Acoustic condensation	1	Inlet of element 1
T	Temperature, K	2	Inlet of element 2, outlet of element 2
t	Time, s	3	Inlet of element 3, outlet of element
U	Propagating sound velocity, $m.s^{-1}$	υ	Relative to the ressonator neck

References

[1] Alster M.: Improved calculation of resonant frequencies of helmholtz resonators, Jornal of Sound and Vibration, Volume 24 (1), pages 63–85, 1972.
[2] Boyce W. E. and DiPrima R. C.: Equações Diferenciais Elementares e Problemas de Valores de Contorno, Ninth edition, Rio de Janeiro, LTC S. A., 2010.
[3] Cai C. and Mak C. M.: Acoustic performance of different Helmholtz resonator array configurations, Applied Acoustics, Volume 130, pages 204–209, 2018.
[4] Collin R. E.: Field Theory of Guided Waves, IEEE PRESS, 1990.
[5] Dourado H. A.: Dicionário de termos e expressões da música, São Paulo, Editora 34, 2004.
[6] ESI Group: Scilab 6.0.2. Avaliable on https://www.scilab.org/, 2019.
[7] Gerges S. N. Y.: Ruído: Fundamentos e Controle, Second edition, Florianópolis, NR Consultoria e Treinamento, 2000.
[8] Hughes T. J. R.: The Finite Element Method: Linear Static and Dynamic Finite Element Analysis, Dover Publications, 2000.
[9] Kinsler L. E., Frey A. R., Coppens A. B. and Sanders J. V.: Fundamentals of Acoustics, New Jersey, John Wiley & Sons, 2000.
[10] Lamb, Horace: The dynamical theory of sound, Second edition, New York, Dover Publications, 1960.
[11] Lopez, A. A.: Estudo comparativo analítico–numérico de vibrações livres e livres acopladas fluido–estrutura em cascas cilíndricas, Master's thesis, Brasília, Universidade de Brasília, 2014.
[12] Panton R. and Miller J.:Resonant frequencies of cylindrical Helmholtz resonators, The Journal of the Acoustical Society of America, Volume 57(6), page 1533, 1975.
[13] Pereira, L. V. M.:Estudo experimental da influência de um ressonador de volume variável na massa de ar admitida por um motor de combustão interna, PhD thesis, Belo Horizonte, UFMG, 2008.
[14] Porges G.: Applied Acoustics, Edward Arnold, 1977.
[15] Seo B. and Chen C.: The relationship between the Laplace transform and Fourier transform, IEEE Transactions on Automatic Control, Volume 31 (8), pages 751–751, 1986.
[16] Song H. S. and Cho H. M.: A study on duct integrated resonator of automobile intake system, Int. Journal of Applied Engineering Reseach, Volume (12), pages 7696–7699, 2017.
[17] Tang P. and Sirignano W.:Theory of a generalized Helmholtz resonator, Journal of Sound and Vibration, Volume 26(2), pages 247–262, 1973.
[18] Vér I. L., Benarek L. L.: Noise and Vibration Control Engineering: Principles and Applications, New Jersey, John Wiley & Sons, 2005.
[19] Weyna S., Mickiewicz W., Pyla M. and Jablonski M.: Experimental acoustic flow analysis inside a section of an acoustic waveguide, Archieves of Acoustics, Volume 38 (2), pages 211–216, 2013.
[20] Williams J.: Laplace transforms, London, Allen & Unwin, 1973.
[21] Yasuda T., Wu C., Nakagawa N. and Nagamura K.: Studies on an automobile muffler with the acoustic characteristic of low–pass filter and Helmholtz resonator, Applied Acoustics, Volume 74 (1), pages 49–57, 2013.

ANNALS of Faculty Engineering Hunedoara – International Journal of Engineering
ISSN 1584 – 2665 (printed version); ISSN 2601 – 2332 (online); ISSN–L 1584 – 2665